Design and Development of Single Material Single Part regenerative combustion chamber

D. Liuzzi and M. Rudnykh**

**AVIO s.p.a., Via Ariana km 5.2, 00034 Colleferro (Rome), Italy*

Corresponding Author: daniele.liuzzi@avio.com

Abstract

In the current worldwide commercial market, product costs and reliability are the most important aspects. This rule is also applicable to the space transportation systems both for launchers and engines. It is important to identify new technological solutions to increase performance, to reduce development cost and to simplify the subsystems architecture. The combustion chamber cost is almost 25-35% of the propulsion system cost, then any upgrading to this element has a direct and significant impact on the engine cost. A promising technology is to change the architecture of the cooling system using innovative solutions devoted to the enhancement of the propellant cooling capability and to the simplification of the manufacturing, using a Single Material Single Part combustion chamber. The feasibility from the manufacturing point of view is guaranteed by the novel Additive Layer Manufacturing technologies. In this paper we focus on the design of the SMSP combustion chambers, describing the Demonstrator development plan. Details are provided on the preliminary design phase and design verification phase by thermo-structural and computational fluid dynamics numerical simulations. Moreover is presented the status on the manufacturing process.

1. Introduction

State of the art most of the regenerative cooled combustion chambers for liquid rocket engines are composed of two main elements: an inner liner made with high conductivity material and an outer shell made with low thermal conductivity material but high mechanical strength. Cooling process and heat extraction takes place through the propellant passage inside the cooling channels, dig in the liner along the entire chamber length. The liner and the outer shell are joined together through various processes. As regards the type of the cooling channels, these have generally a rectangular section that allows to maximize the structural strength of the liner and the heat extraction capability. The new cooling system concept has the main purpose to increase the heat exchange by convection on the cold side through reticular and ordinated structures that increase the turbulence and destroy the fluid stratification into the coolant passage section. The last one is not more a rectangular channel but an open annular area where the fluid is guided by the reticular structures orientation, which have the role to ensure the structural integrity of the chamber retaining the ability to sustain pressure and thermal loads by connecting the outer shell with the inner liner. The new combustion chamber concept also foresee to simplify the architecture using only one material for liner, reticular structures and outer shell, moreover to obtain the final system with a Single Material and a Single Part. The feasibility of this combustion chamber is linked to the utilization of the novel ALM technology that allows to build complex geometries starting from the material powder. The feasibility study [3], performed for this combustion chamber, highlights that it is possible to obtain the same performance by the new combustion chamber respect to a traditional configuration.
The development plan for the DEMO SMSP combustion chamber has been divided in different phases with different test articles, each one is devoted to do a step forward in the set-up of the design and technological processes. The first phase is to investigate the ALM limits in terms of dimensional and shape tolerances that is possible to obtain, some details are provided in the following. In the second phase a cylindrical module with a traditional cooling system concept was designed and manufactured with the scope to validate by a firing test the feasibility of the combustion chamber with ALM. The third one consists in the design and testing of the reticular structures that composes the innovative cooling system concept, with the main scope to estimate by cold test the hydraulic resistance of these structures and to validate the CFD DNS simulations. The forth step is the design and testing of the cylindrical module with the innovative cooling system, in order to validate the design hypothesis and to confirm the increase of the cooling capability of this new concept before the implementation on the chamber nozzle. The fifth phase consists in the design and testing of the nozzle module characterized by the highest heat fluxes along the chamber, the success of this phase allows to proceed with the design of the DEMO SMSP combustion chamber.
In this paper we focus on the second phase of the activity, describing the design choices and methodologies, starting from the feasibility design up to the thermo-structural and fluid dynamic verification. The preliminary design describes the design choices that led to the SMSP TA01 geometry definition, performed with Q-1D methodology and the

performance estimation process. The thermo structural verification is performed by a 3D-FEM simulation and the fluid-dynamics behavior is estimated by a 3D-CFD simulation. It is also described the test article, the instrumentation used for the experimental measurements and some aspect of the manufacturing process.

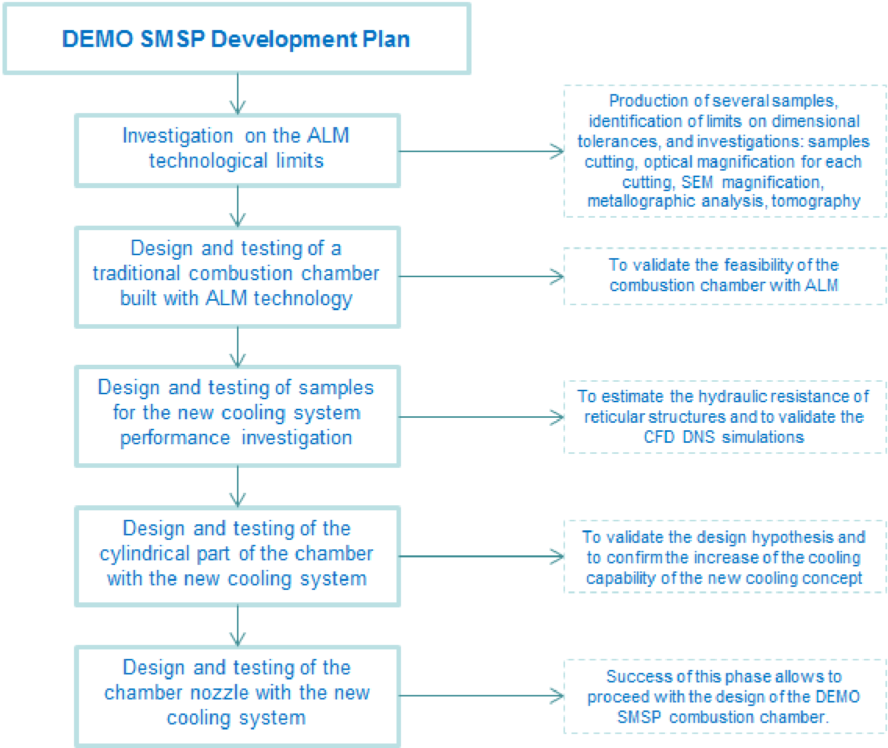

Figure 1: SMSP Development plan.

2. Experimental testing and test hardware

The firing test will be conducted using liquid oxygen and gas methane in the FAST2 AVIO test stand [2]. The experimental investigation is performed using the KeRC combustion chamber. This chamber was developed by the Keldysh Research Center during AVIO self-funding activities, and it was used to set-up the FAST2 test stand and successively for the sub-scale tests of the injection head developed for the MIRA engine in frame of the LYRA program test campaign. The KeRC chamber is a modular combustion chamber, showed in Figure 2, built with traditional manufacturing technique using a copper alloy liner and steel alloy close-out. It is characterized by four parts: the injection head module, the ignition module, the cylindrical module and the nozzle module. Each module has its own water cooling system. The SMSP test articles corresponding to each development phase are characterized by the same overall dimensions and interfaces of the KeRC modules, during the tests them will be substituted between each other.

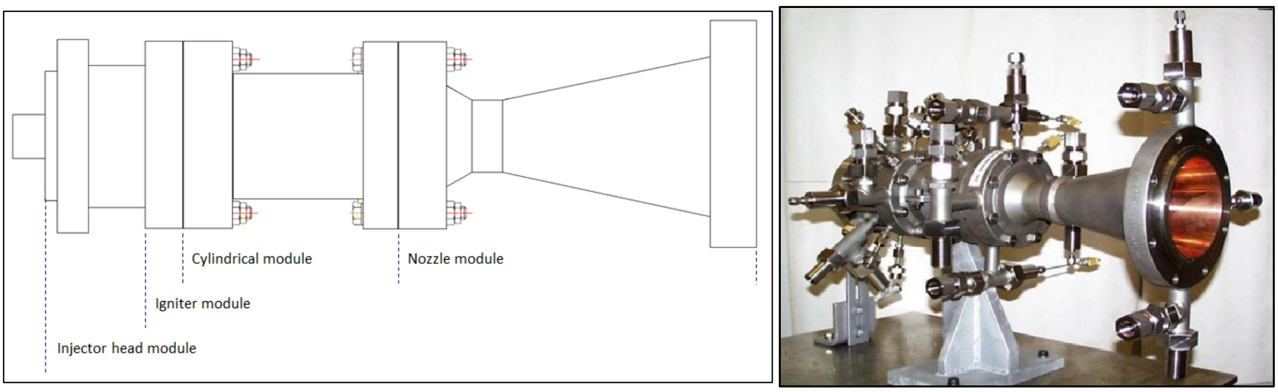

Figure 2: KeRC Thrust Chamber Assy.

3. Combustion Chamber Design

The combustion chamber internal geometry is the same of the KeRC one, propellants are liquid oxygen and gas methane for a nominal combustion pressure of 50 [bar] with 3.4 [-] mixture ratio. The combustion products condition and properties are estimated with the CEA code for chemical reaction calculation [1], considering frozen mixture composition. Results are shown in Figure 4, for gas pressure, temperature and dimensionless number of Prandtl and Reynolds. The cylindrical module design follows three design steps: feasibility phase, optimization phase and verification phase. The feasibility design is skipped because the overall dimensions are linked to the AVIO existing combustion chamber. The optimization phase is carried out by means of an in-house AVIO Q-1D code that solves for the fluid-dynamic conservation equations of the coolant fluid and it provides the cooling jacket performance in term of fluid properties along the chamber length and chamber walls temperature. The verification design phase consists of a thermo-structural 3D simulation made with the commercial code MARC, and a 3D-CFD simulations made with the commercial code Fluent; these are used to confirm the structural integrity of the combustion chamber and the fluid conditions inside the cooling channels. All plots in the following are dimensionless with respect to chamber length and main operative point.

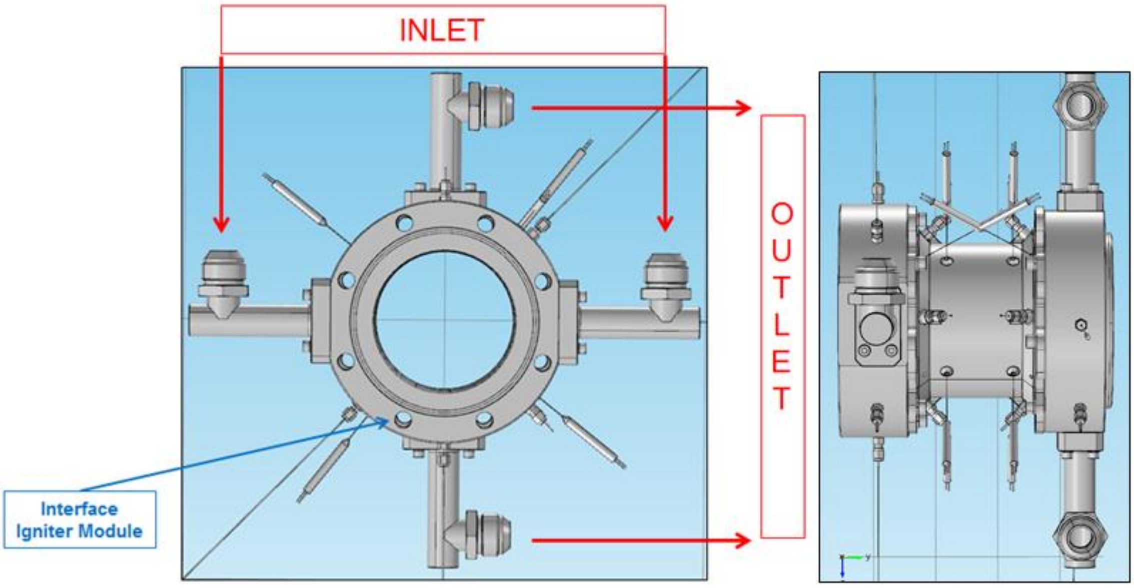

Figure 3: Test bench interfaces.

3.1. Cooling system dimensioning

The optimization process is performed changing the design parameters in order to obtain the required performance. In particular for water cooling it is very important that the coolant does not change phase from liquid to vapor on the cold side liner wall. To this aim the liner temperature should be low enough that the saturation pressure is significantly lower than the fluid pressure in the channel. The difference between these pressure values is named here “saturation margin” and it is shown in the last two diagram of Figure 5 where the left one is the water phase diagram and the red curve represents the cold side liner temperature, the right one directly shows the percentage margin value along the chamber. The saturation margin reference value comes from our experience with the MIRA combustion chamber performance estimation. The liner thickness and the rib width are chosen accordingly to the feasibility investigation activity for the estimation of the minimum feasible value obtained by the additive layer manufacturing.
Because the scope of second phase is to verify the feasibility of a combustion chamber made by ALM, we chose a safe nominal operating point characterized by a saturation margin of 3 times higher than the reference value.
In the following figures the heat flux, temperature and pressure are dimensionless with respect the corresponding maximum value.

3.2. Thermo-structural verification

The simulation model takes into account a 3D angular portion of the chamber taking advantages by its axisymmetric geometry, Figure 6. The angular portion includes the thicker ribs where the thermocouples are inserted to measure the liner temperature, Figure 9. The geometry is composed by the liner, the close-out and the inlet manifold, needed to simulate the interface connection with the igniter module. The simulations are nonlinear and it takes into account for plastic behavior of the material, material properties dependency by temperature and contact between bodies to simulate the joining zone. The mesh is structured all along the liner and the close out is structured on the boundaries and free quadrilateral are used to close the internal zone. The MARC software has been used for the simulation.

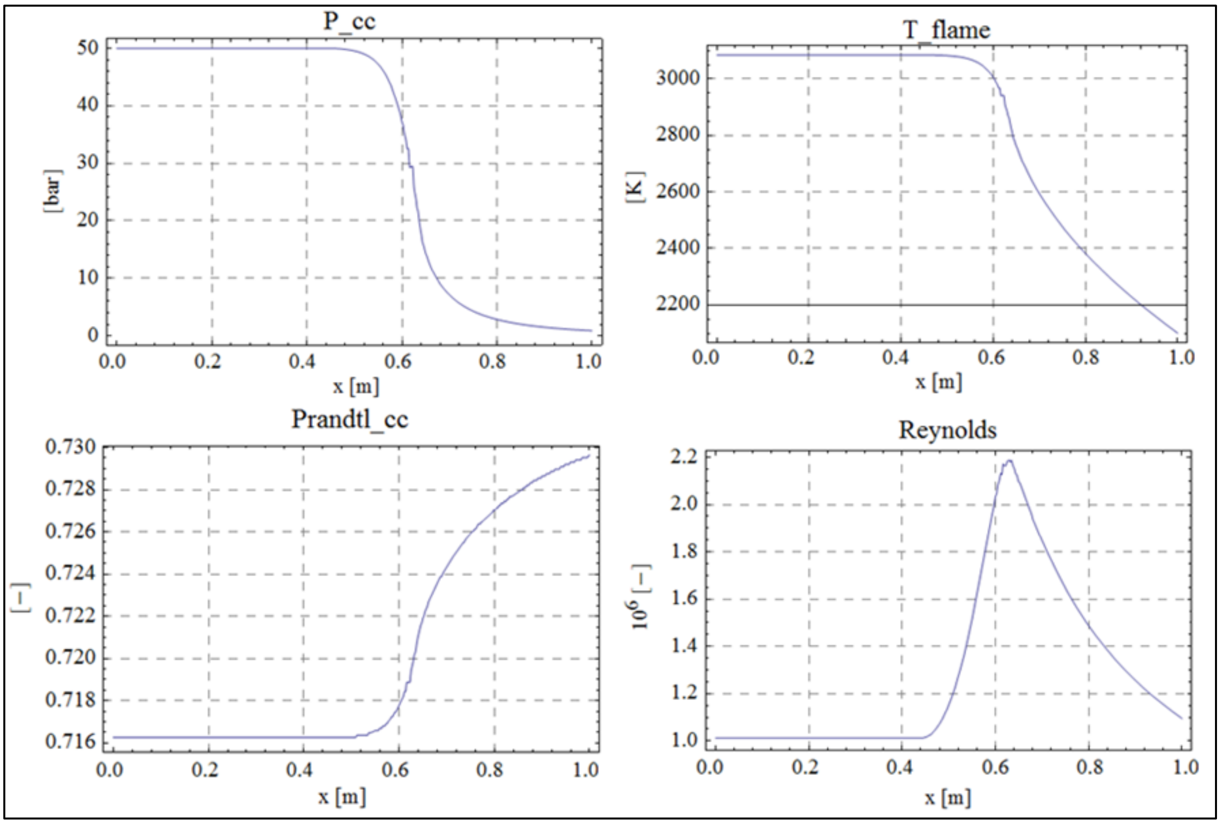

Figure 4: TCA hot gas side conditions.

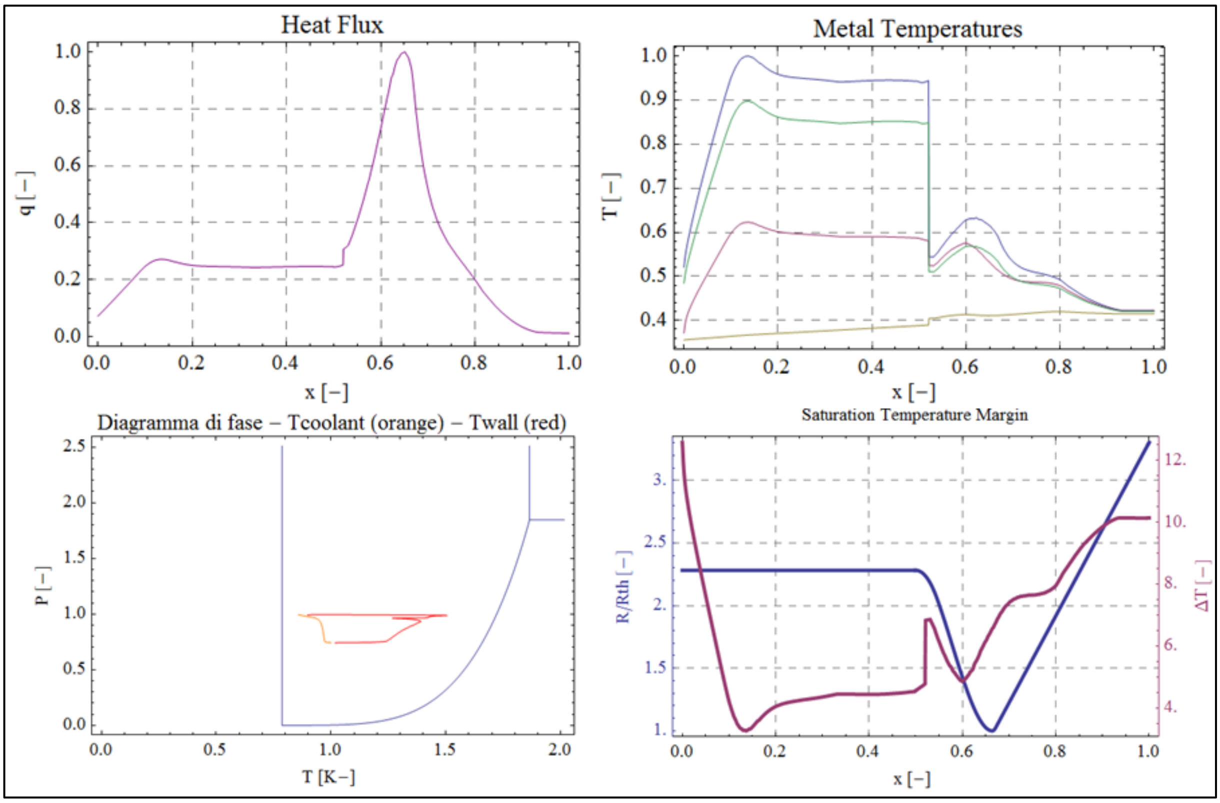

Figure 5: Cooling system performance.

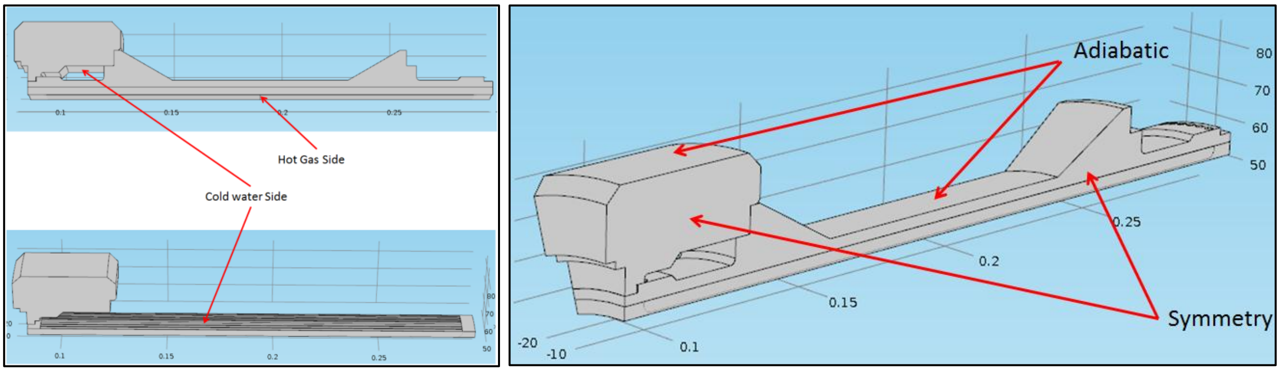

Figure 6: FEM model, geometry and boundary conditions.

The simulation is time dependent in order to investigate the test operative cycle of the combustion chamber in Figure 7, it starts from the ignition t=0 [s], to the first step at 20% of combustion condition, up to the 100% operative condition. Following this phase there is the shut-down and the simulation of the cooling phase with natural convection. The percentage of load is properly applied to all the boundary conditions. Cyclic symmetric BC is used on the lateral surfaces of the geometry and adiabatic thermal insulation is considered for the close-out surface against the external environment, Figure 6. On the hot gas zone is used the heat flux and pressure, while on the fluid side the convective heat exchange coefficient, temperature and pressure, showed in Figure 5. The plasticization curves are obtained by yield and ultimate allowable that are estimated by tensile tests curves.

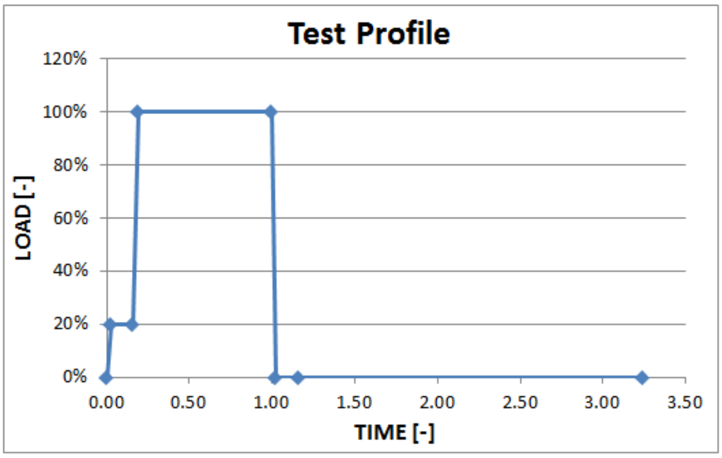

Time [s]	Load [-]
0.00	0%
0.03	20%
0.16	20%
0.19	100%
1.00	100%
1.03	0%
1.16	0%
3.24	0%

Figure 7: Margin respect to water vaporization on cold side wall.

The simulations have been conducted for three geometries characterized by different channels number, from 89% to 111% of the reference number and different rib thickness, twice the reference one. In particular the thicker rib has been introduced to allows the thermocouples positioning in the test article. FEM results show good agreement with the Q-1D performance prediction and no critical behaviour are highlighted in term of temperature or stress. For the reference geometry the safety factor are always greater than 1.37 [-], both for the yield than for the ultimate stress, Table 1. Temperature maps respectively for the zone close to the water inlet and for the cylindrical zone are showed in Figure 8. The investigation on the rib thickness is showed in Figure 9, two configuration have been investigated with different ribs number to highlight possible criticality, on the left side is the geometry with minimum number of channels and on the right the one with the maximum number. Results are summarized in Table 2, where data are provided for six points inside the liner, in particular in the channel, below the nominal rib and below the thicker rib, both on the cold side and hot gas side walls. It is interesting to notice in Table 2 that the safety factor at the rib center is lower in the case of higher ribs number, then with a minor spacing. This is because the structure is more constrained and the stress is dominated by the thermal effect. Temperature in the following tables is dimensionless with respect to the maximum liner temperature on the hot gas side.

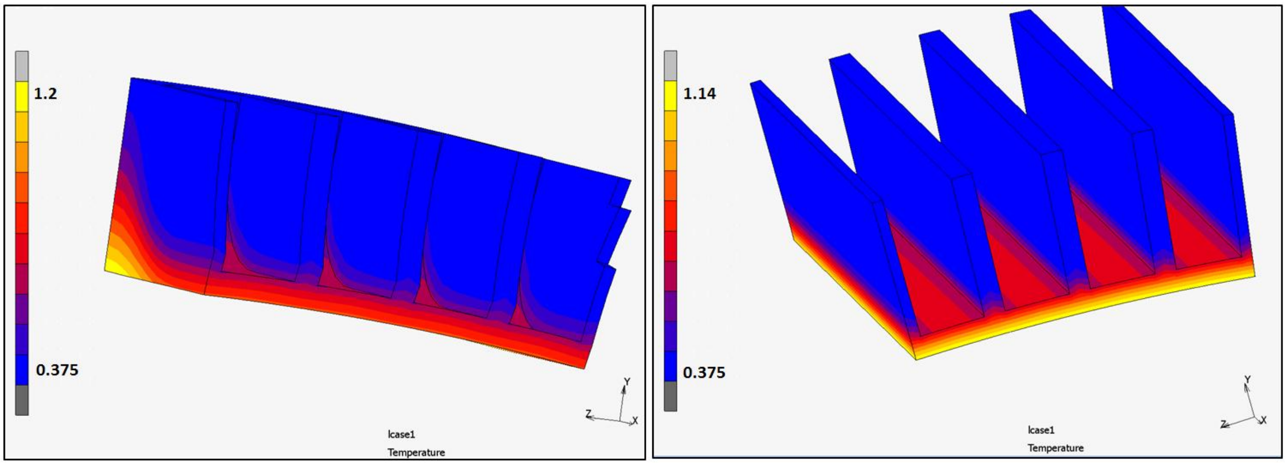

Figure 8: Temperature maps – Details on water inlet zone and cylindrical zone.

Position		T/Tmax [-]	VM [MPa]	SF ultimate	SF yield
x=0 [-]	Tmax	1.198	640	1.64	1.46
x=0.01 [-]	liner water side	0.63	604	2.13	1.79
x=0.01 [-]	liner gas side	0.895	690	1.79	1.52
x=0.08 [-]	liner water side	0.691	781	1.64	1.37
x=0.08 [-]	liner gas side	1.14	643	1.73	1.52

Table 1: Detail 1 Safety factors, position referred to indication on Figure 8.

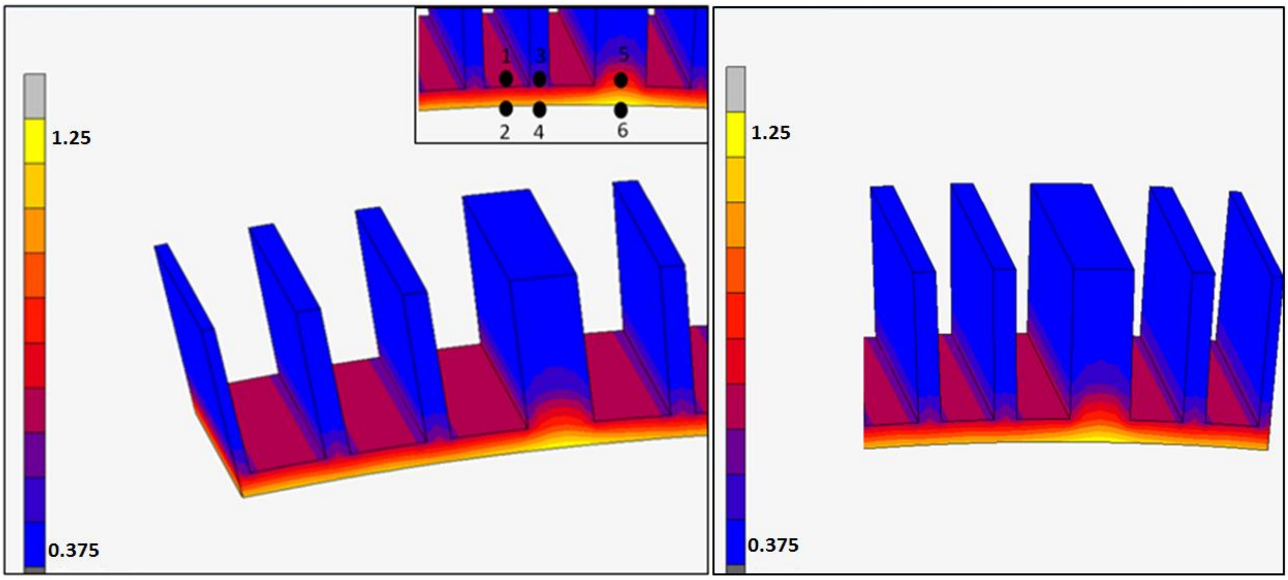

Figure 9: Investigation with different ribs number.

Ribs	Position		T/Tmax [K]	VM [MPa]	SF ultimate	SF yield
89%	Channel center	liner water side (1)	0.683	742	1.72	1.45
		liner gas side (2)	1.129	690	1.62	1.43
89%	Rib center	liner water height (3)	0.674	425	3.01	2.53
		liner gas side (4)	1.110	696	1.63	1.43
89%	Thicker Rib center	liner water height (5)	0.905	517	2.39	2.02
		liner gas side (6)	1.250	582	1.67	1.52
111%	Channel center	liner water side (1)	0.675	776	1.65	1.39
		liner gas side (2)	1.113	690	1.64	1.44
111%	Rib center	liner water height (3)	0.674	434	2.95	2.48
		liner gas side (4)	1.108	696	1.63	1.43
111%	Thicker Rib center	liner water height (5)	0.906	513	2.41	2.04
		liner gas side (6)	1.243	582	1.69	1.53

Table 2: Details 2 Safety factors, position referred to indication on Figure 9.

3.3. Fluid Dynamic verification

Taking advantage from the axisymmetric geometry of the combustion chamber, the computational domain has been reduced to two adjacent channels: the imposed boundary conditions are the heat flux on the hot gas side wall, the adiabatic condition on the upper wall and the periodic condition on the lateral walls. Moreover, inlet and outlet conditions for the fluid are imposed. The boundary conditions and the computational domain are showed in Figure 10.

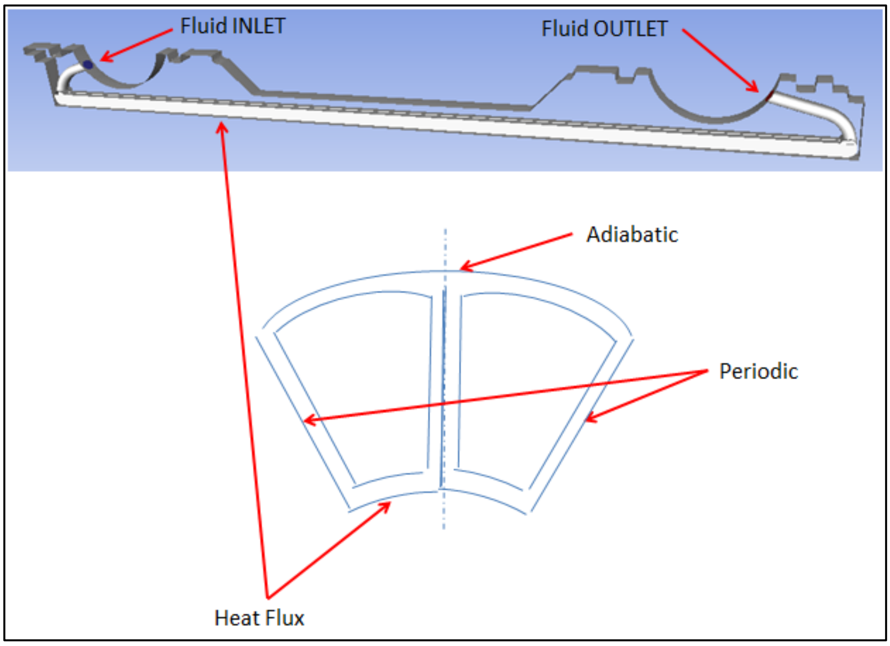

Figure 10: Computational domain and BCs and simulation control positions.

The contour plot in Figure 11 shows the velocity field of the coolant inside the channels; the velocity profile is almost uniform in the computational domain, except in the inlet and outlet zones that are detailed in Figure 12. We noticed the generation of small recirculation area in the upper zone of the channel, and an acceleration of the fluid in the lower zone of the channel, due to the duct curvature and restriction of the channel section. For the outlet zone of the cooling channel, a similar phenomenon can be observed: the slowing of the fluid along the lower wall, and the acceleration of the fluid in the upper zone, due to the sudden curvature of the outlet duct. These phenomena does not have a significant impact on the cooling capability of the system. The fluid temperature and velocity with respect to the y axis of the chamber, for 5 axial positions are shown in Figure 13. On the left picture the fluid velocity profiles vs. radial position, despite the irregular profile corresponding to the first position close to the recirculating zone, the other 4 four profiles show a fully developed flow with boundary layer. On the right picture the fluid temperature profiles vs. radial position inside the channel from the liner water side to the close out side, illustrates how the temperature gradient along the y axis increases proceeding towards the end of the channel, indicating an increasing stratification of the fluid temperature. Clearly the temperatures are higher near the liner and for greater values of the abscissa.
Wall temperature profiles are showed in Figure 14, and evaluated in 4 interesting positions, that are hot gas side of the liner, cold side of the liner, rib base and rib half height. Temperatures are influenced by the velocity profile: they reach the minimum values in correspondence of the fluid reattachment after the inlet duct, and they reach the maximum values in correspondence of the channel outlet, where the liner thickening, together with the effect of the sudden curvature, decreases the heat transfer between chamber and coolant, leading to the maximum liner temperature that is however much lower than the material allowable.
The coolant temperature increases linearly from the inlet to the outlet section. The coolant pressure values along the channel estimated with Fluent have been compared with the prediction of the experimental Nikuradse correlation, showing good agreement and a maximum error on the pressure drop of + 1.79%.
The 3D-CFD verification activity highlighted good agreement with the Q-1D code estimation and it was particularly useful to verify the chamber integrity in the critical zone, located in the recirculating zones close to the outlet section.
In the following figures the velocity and temperature are dimensionless with respect the corresponding maximum value.

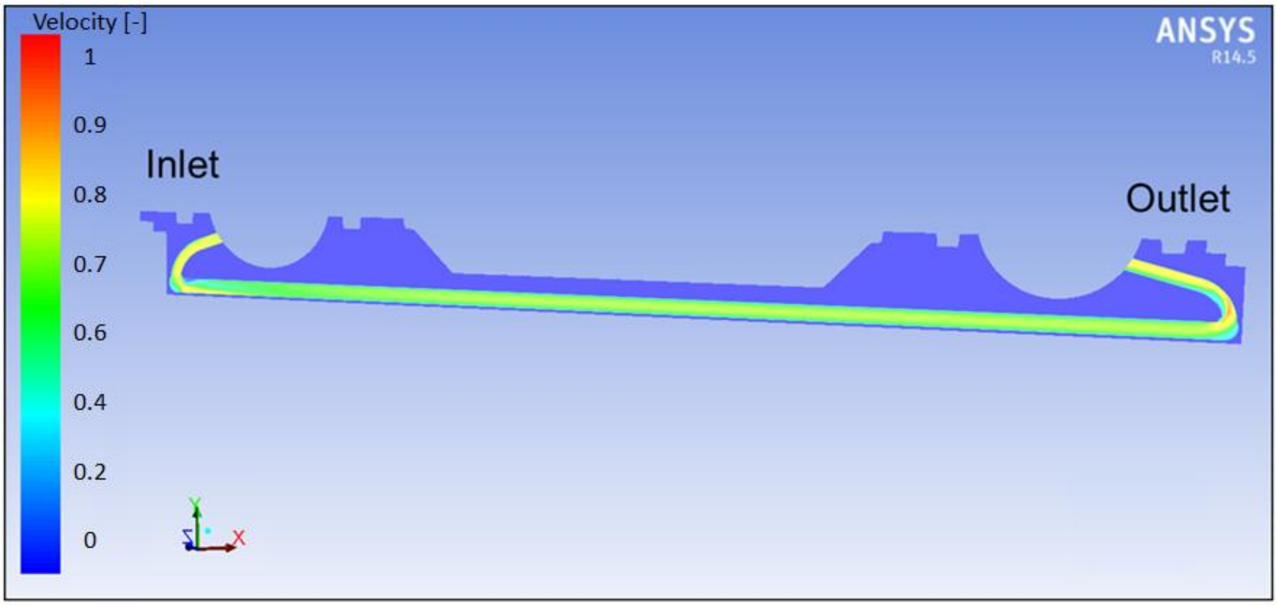

Figure 11: Velocity field inside the cooling channels.

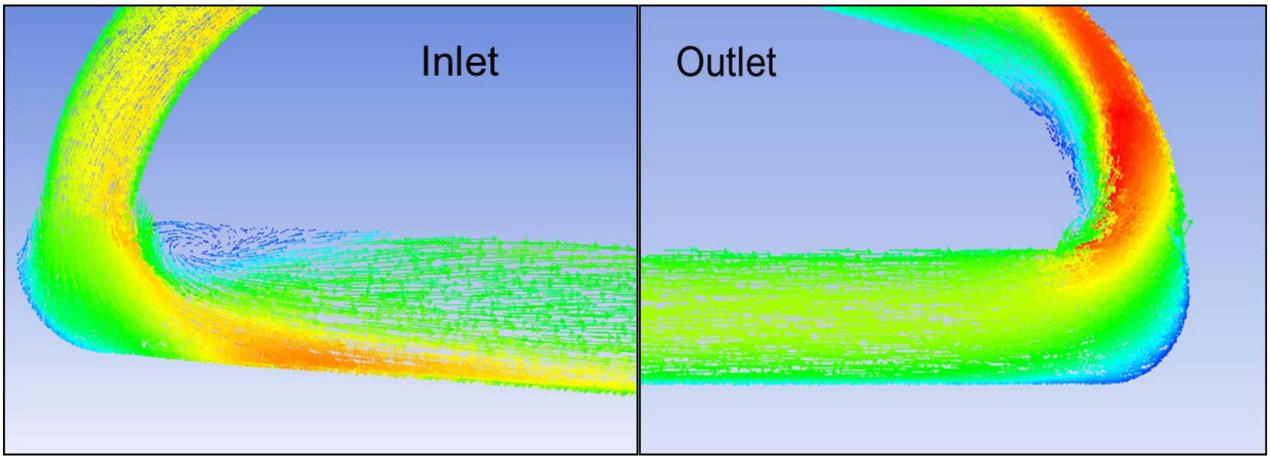

Figure 12: Detail of inlet and outlet velocity field.

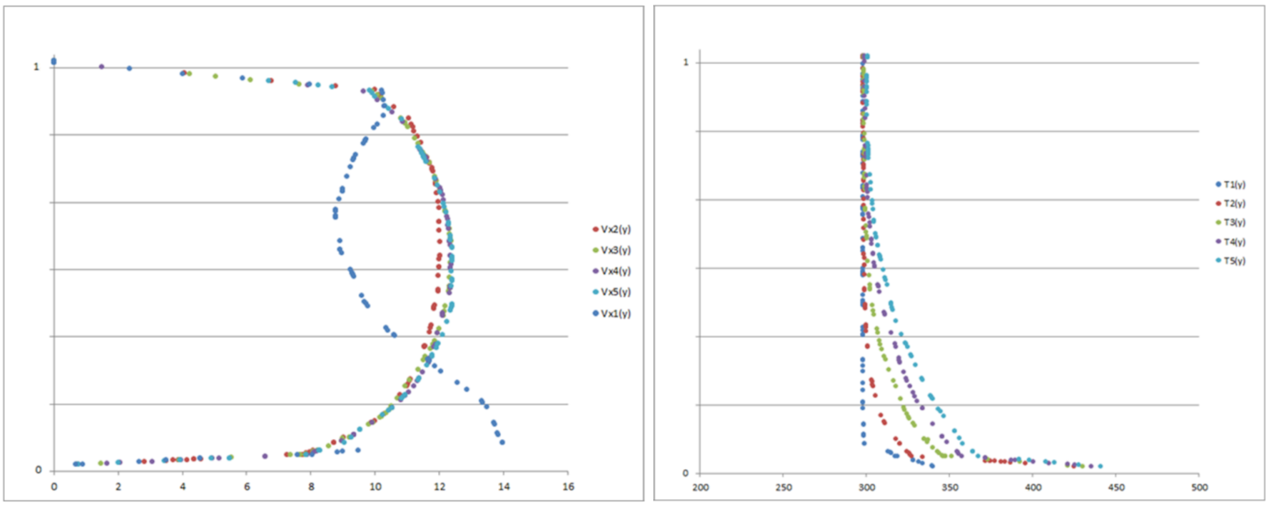

Figure 13: Axial velocity and fluid temperature profiles [K] vs. radial position [m].

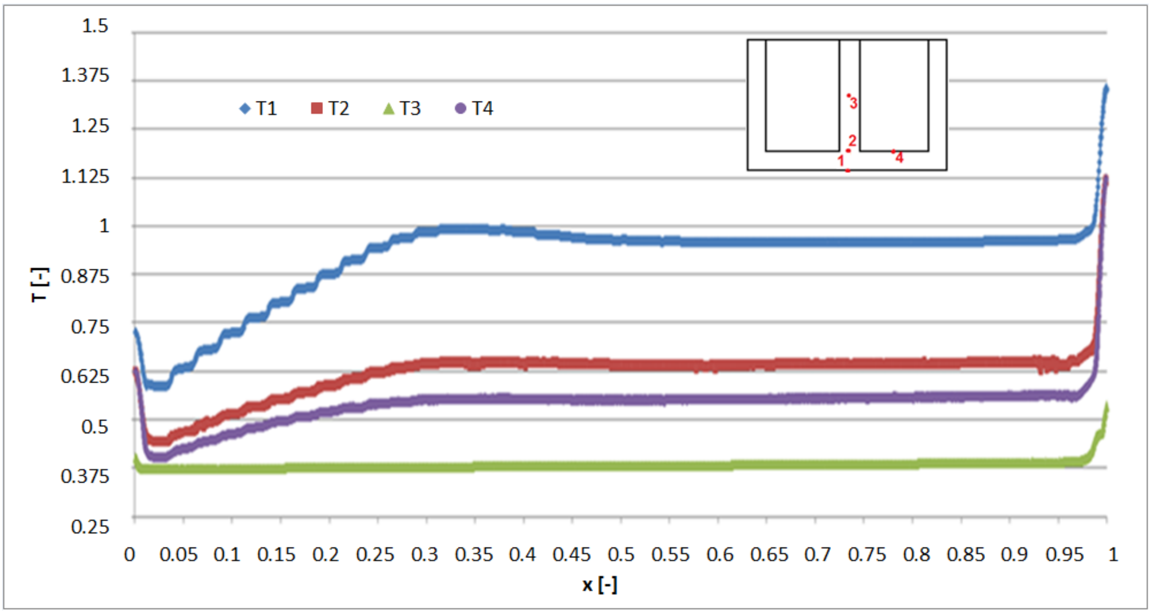

Figure 14: Metal temperature profiles vs. axial position.

4. Instrumentation

To fully understand the phenomena involved in this kind of application and to confirm the design methodology, the test article is instrumented with pressure transducers and thermocouples, as shown in Figure 15. In particular the following measuring point are located on the test article:

- Inlet manifold pressure (2 measuring points).
- Inlet manifold temperature (2 measuring points).
- Outlet manifold pressure (2 measuring points).
- Outlet manifold temperature (2 measuring points).
- Cooling system inlet pressure (4 measuring points).
- Cooling system outlet pressure (4 measuring points).
- Liner metal temperature close to combustion surface (16 measuring points).

The cooling system pressure measurement are positioned close to the inlet and outlet section. The liner metal temperature are inserted into the liner rib and are positioned as close as possible to the hot gas wall.

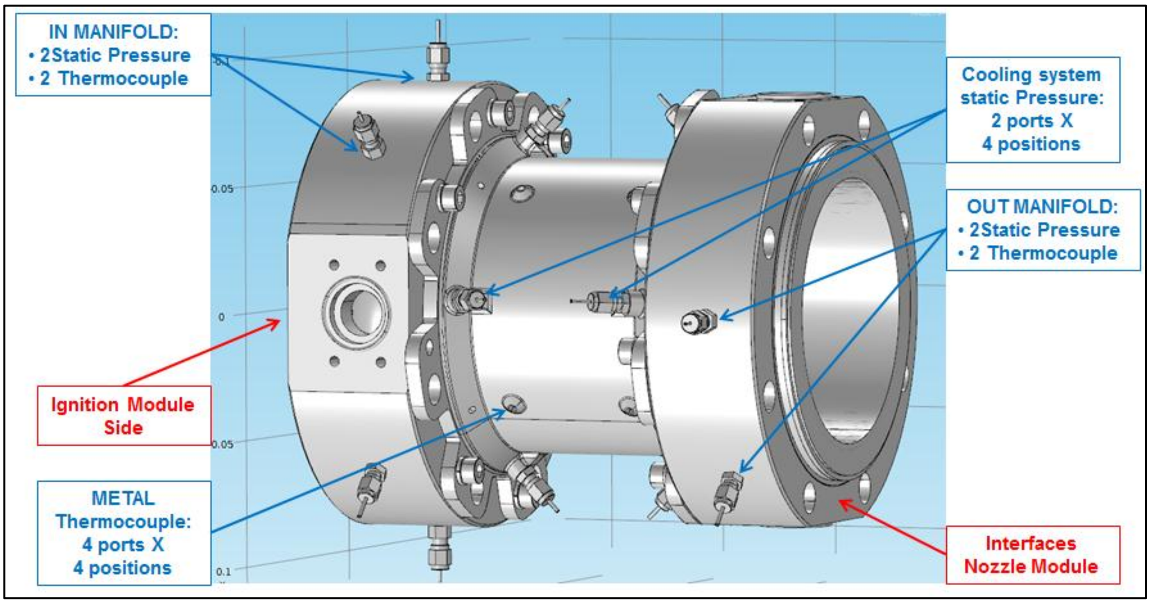

Figure 15: Test article instrumentations.

5. Manufacturing

With regard to the manufacture, two metallic powder laser fusion technology have been chosen for SMSP manufacturing: provided by Consept Laser and Renishaw machine. The choice has been based on preliminary technical assessment to produce the chamber by Inconel 718 and also on the base of economic offer of the machine owners. The general characteristic of the machine used for are summarized in below:

	CONCEPT LASER	**RENISHAW**
Machine model	M2 Cusing	AM 250
Building Volume	250 X 250 X 280 mm (17.500 cc)	245 X 245 X 360 mm (21.600 cc)
Laser power	200 o 400 W	200 o 400 W
Scanning Vmax	7 m/s	2 m/s
Layer thickness	20 - 80 micron	20 - 100 micron

Table 3: General characteristics of ALM machines.

In the first phase of the development plan we investigated the ALM limits in terms of dimensional and shape tolerances that is possible to obtain, we produced several samples like cylindrical angular portion of the chamber, converging-diverging-nozzle and reticular structures for the innovative cooling system concept, Figure 16. Different thickness of the liner and ribs have been produce in order to define the best capability of the technology. Also the first attempt of a reticular structure has been realized with different thickness. For each sample was conducted control investigations as: samples cutting, optical magnification for each cutting, SEM magnification, metallographic analysis and finally tomography for inclusions identification and for the control of not accessible zones.

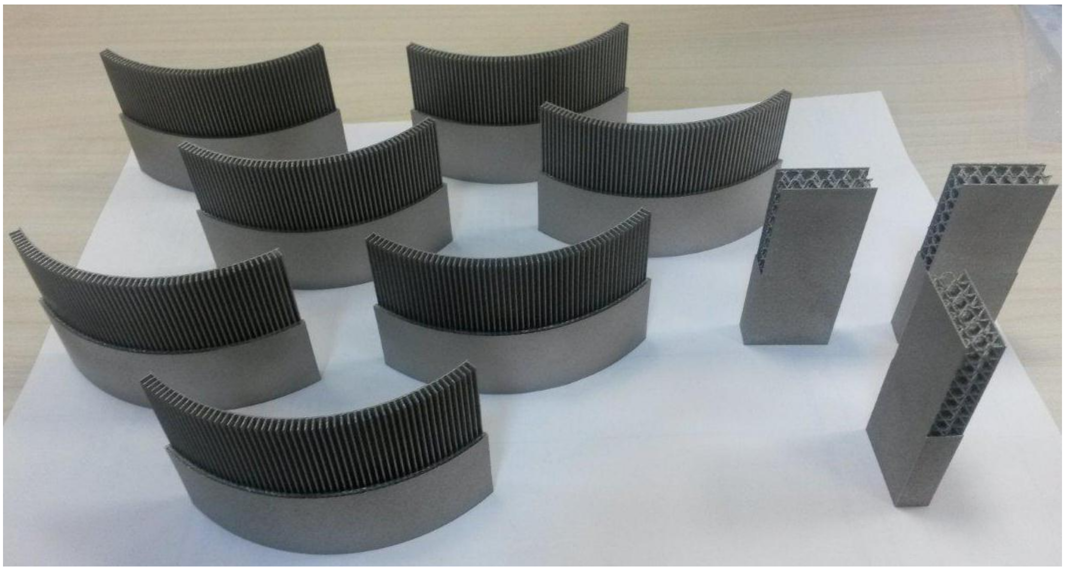

Figure 16: First job activity – feasibility investigation.

In the Figure 17 the second job feasibility verification samples are presented. There were investigated the stability of the thickness and tolerances in the more complicated structures.

Figure 17: Second job activity – feasibility verification.

Another important activity performed is the validation of non-destructive inspection technics of the critical geometrical dimensions, which are not available for the direct controls. In order to verify the measure internal dimensions and to have an evidence that internal cavities are free of powder residuals, the tomography inspection has been applied on the sample represented the real diameter of cylindrical module, left Figure 18. After that, the sample produced has been mechanically cut at the same section used for tomography inspection and direct measurement controls has been done, right Figure 18. In such way the acceptable level of accuracy of the tomography inspection has been confirmed. Some images of the NDI controls are presented in Figure 19. To be noted, that also some samples for mechanical finishing have been produced.
Following the positive results of the preparation activities performed during the first phase, the SMSP cylindrical modules have been produced. The SMSP prototype is characterized by a length of 210 [mm] and a maximum diameter of 180 [mm]. These dimensions were challenging for both the machines providers, Consept Laser and Renishaw. To be noted that both of them successfully accomplished cylindrical module manufacturing. In Figure 20, there is the SMSP prototype CAD model compared with the module produced by Concept Laser machine with technological supports.

Figure 18: SMSP prototype, NDI validation sample.

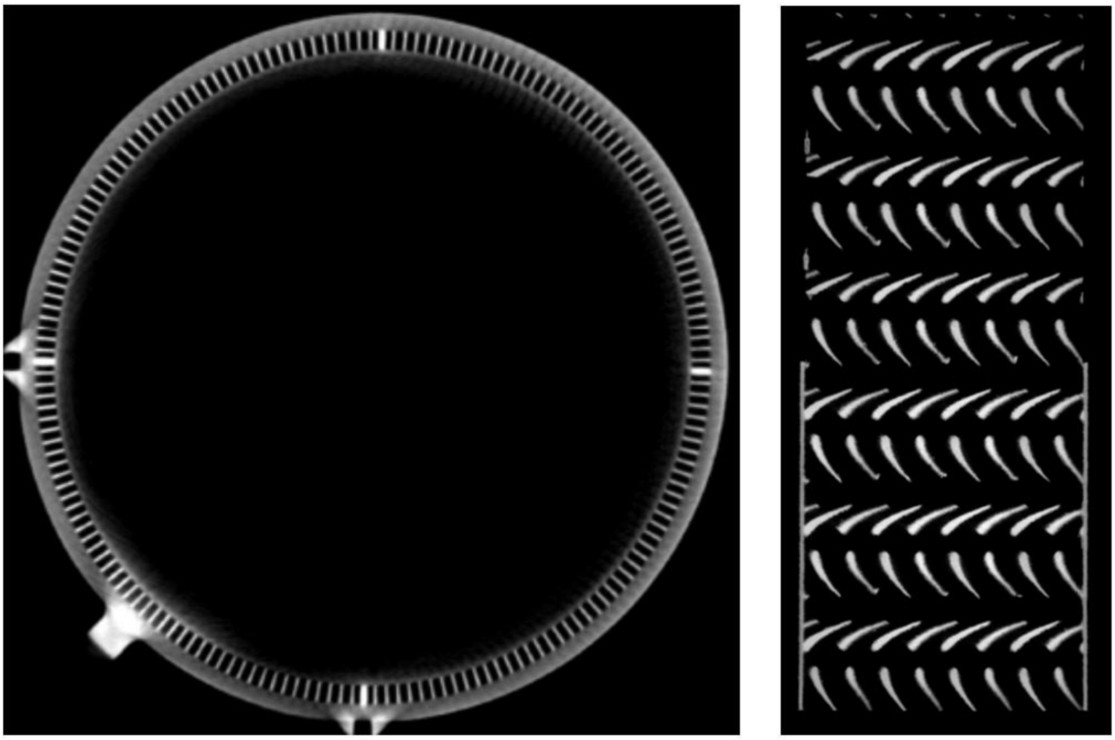

Figure 19: SMSP prototype, NDI controls – left cylinder, right reticular structure.

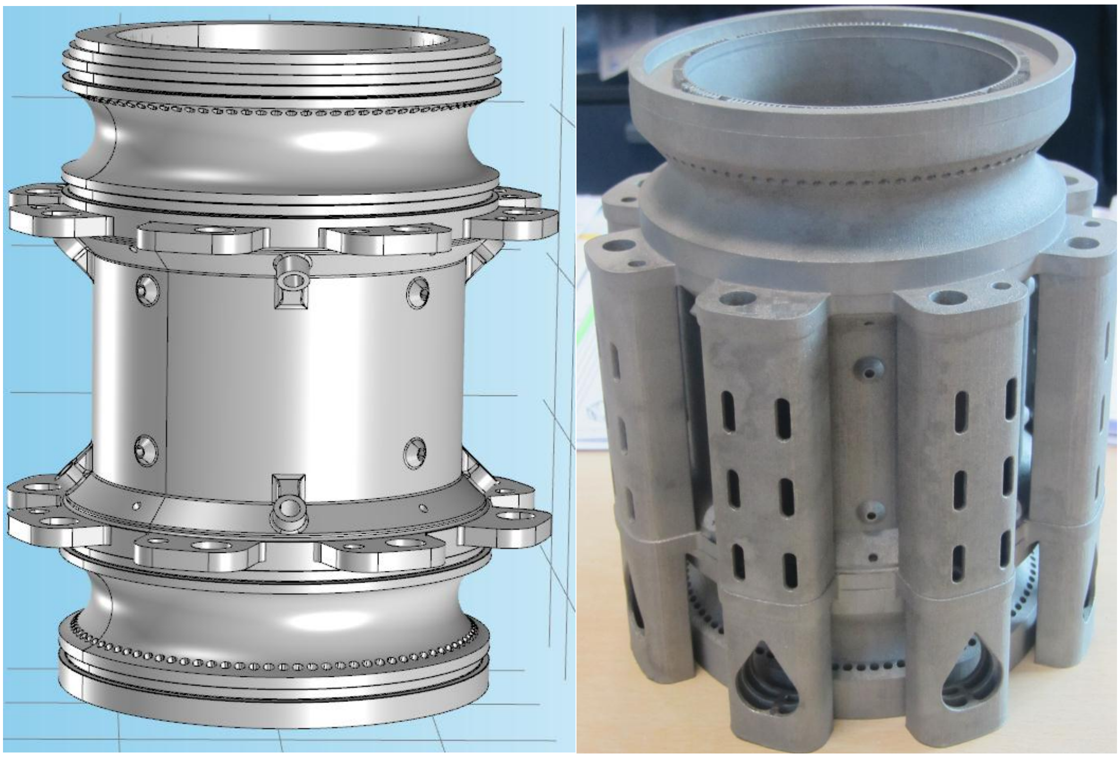

Figure 20: SMSP prototype, TCA cylindrical module.

6. Conclusion

The SMSP program consist in the development of an innovative combustion chamber made with only one material Inconel 718 and only one part that includes both liner and close-out. We accomplished the first and second phase of the program development plan up to the manufacturing level. It allowed as to set-up the design procedures and the design verification phase made by numerical simulations. We deeply investigated the Additive Layer Manufacturing technology identifying the process feasibility and limits in term of maximum and minimum dimensions, manufacturing tolerances and not destructive controls. The next step is to perform within 2015 the firing test with the SMSP cylindrical module that allows to obtain the first experimental validation. Currently we began the third development phase and we foresee also to characterize experimentally the reticular structure performance within 2015.

7. Nomenclature

ALM	Additive Layer Manufacturing
CFD	Computational Fluid Dynamic
FEM	Finite Element Method
KeRC	Keldysh Research Center
NDI	Non Destructive Inspection
SMSP	Single Material Single Part
TCA	Thrust Chamber Assy

8. References

[1]. “Computer Program for Calculation of Complex Chemical Equilibrium Compositions and Applications”, S. Gordon e B. J. McBride, Cleveland, 1994.

[2]. “LYRA Program: LOx-CH4 firing test activities at FAST2 stand”, D. Scarpino, N. Ierardo and A. Ferretti, Space Propulsion, 2010.

[3]. “Single Material Single Part Regenerative Combustion Chamber”, D. Liuzzi and M. Rudnykh, Space Access, 2014.